Kinetic Parameter Estimation of a Commercial Fe-Zeolite SCR

ARTICLE *in* INDUSTRIAL & ENGINEERING CHEMISTRY RESEARCH · JANUARY 2011

Impact Factor: 2.59 · DOI: 10.1021/ie101558d

7 AUTHORS, INCLUDING:

Tae Joong Wang
Doosan Infracore
9 PUBLICATIONS **84** CITATIONS
SEE PROFILE

Seung Wook Baek
Korea Advanced Institute of Science and Tec…
243 PUBLICATIONS **2,022** CITATIONS
SEE PROFILE

Hyuk Jae Kwon
Samsung Advanced Institute of Technology
45 PUBLICATIONS **895** CITATIONS
SEE PROFILE

Young Jin Kim
Chonnam National University
658 PUBLICATIONS **6,636** CITATIONS
SEE PROFILE

energy&fuels

ARTICLE

pubs.acs.org/EF

Investigation of NO_x Reduction in Fuel-Lean Reburning System with Propane

Hak Young Kim and Seung Wook Baek*

School of Mechanical, Aerospace and System Engineering, Division of Aerospace Engineering, Korea Advanced Institute of Science and Technology, 373-1 Gusong-Dong, Yusung-Gu, Daejon 305-701, Korea

ABSTRACT: In this study, the fuel-lean reburning system is considered for reducing NO_x emission by using an experimental and numerical approach in conjunction with a lab-scale furnace. Liquefied petroleum gas (LPG) is used as the main and reburn fuel. The goal of this work is to obtain the most optimal combustion system by employing the fuel-lean reburning system to reduce environmental pollution. The amount of reburn fuel and injection location of reburn fuel are considered as experimental parameters. There are very few studies that have focused on how the reburning process is affected by changes in the flow field that are induced by combustion. It is important to study the effect of the combustion condition on the reburning process in order to control fuel-lean reburning. A computational fluid dynamics (CFD) model is used to provide understanding of the complex combustion phenomena. The validation of the predicted results is carefully conducted by comparing the predicted results with the measured data such as species concentration and temperature distribution inside the furnace region. The measured results show that the fuel-lean reburning method leads to 50% NO_x reduction by using a ratio of reburn fuel to total fuel of 0.13 and by achieving complete combustion without any additional oxidizer. In addition, predicted results indicate that the recirculation flow into the furnace region is carefully considered in order to enhance the reburning efficiency.

1. INTRODUCTION

Atmospheric pollution can have serious consequences on the health of human beings as well as on natural ecosystems. In particular, CO, SO_x, and NO_x have been noted as the most hazardous air pollutants due to the massive production from combustion processes, such as coal and gasified fuel fired boilers. However, stringent restriction on the use of fossil fuel is not simple, because it plays an important role in global energy supply.

Mechanisms that govern the formation and destruction of nitrogen oxides have long been studied by many researchers.[1−5] Over the past decade, several methods for controlling the generation of toxic gases have been proposed based on many experimental and numerical investigations. Through unceasing efforts by many researchers[6−8] various technologies have been developed and successfully applied to many industrial circumstances. Among other technologies for NO_x reduction, the reburning process is one of the most widely known technologies that can limit nitrogen oxides ($NO + NO_2 = NO_x$) generation in the combustion process, since it can be easily adapted to conventional industrial combustion systems. The effectiveness of the reburning process is dependent on numerous factors including the local mixing and stoichiometry in the reburning zone.[8] A variety of fuels have been tested for reburning, including coal, biomass, heavy fuel oil, and natural gas.[8−13]

In this study, fuel-lean reburning is considered for reducing NO_x and CO emission. Liquefied petroleum gas (LPG) is used as the main and reburn fuel. The fuel-lean reburning system had been proposed by Energy System Associates (ESA). ESA reported that the fuel-lean reburning technology was expected to achieve 35−40% NO_x reduction with only 7% reburn fuel (as a fraction of the total heat input) without significant modification in the primary combustion zone.[14,15] Miller et al.[16] indicated that in general fuel-lean reburning could be the most effective for the full-scale systems because of the existence of locally fuel-rich regions in these large combustion systems. The effectiveness of fuel-lean reburn system had been also reported by Breen and Hura.[17]

A main difference between the conventional reburning system and the fuel-lean reburning system resides in the fact that the fuel-lean reburning system always maintains an overall fuel-lean condition (equivalence ratio less than 1) in the whole reaction zone, including the reburning zone. Therefore, the burnout zone, which is generally used to carry out complete combustion after the reburning process, is no longer necessary. Usually, adopting an additional air supply zone requires extra injection equipment to be installed, which can result in increasing operating and maintenance costs. Another problem of using additional air is that a significant portion of HCN, which is generated from chemical reactions between hydrocarbon radicals and nitrogen oxides, oxidizes to NO in the burnout zone, which limits the overall NO reduction efficiency. In this respect, the fuel-lean reburning system has a possibility of achieving greater effectiveness than the conventional reburning process.

The goal of this work is to examine the most appropriate combustion condition by employing the fuel-lean reburning system for reducing NO_x emission. Furthermore, there have been very few studies that focused on how the reburning process is affected by changes in the flow field induced by primary combustion. So, it is therefore another important goal of this

Received: June 13, 2010
Revised: January 24, 2011
Published: February 20, 2011

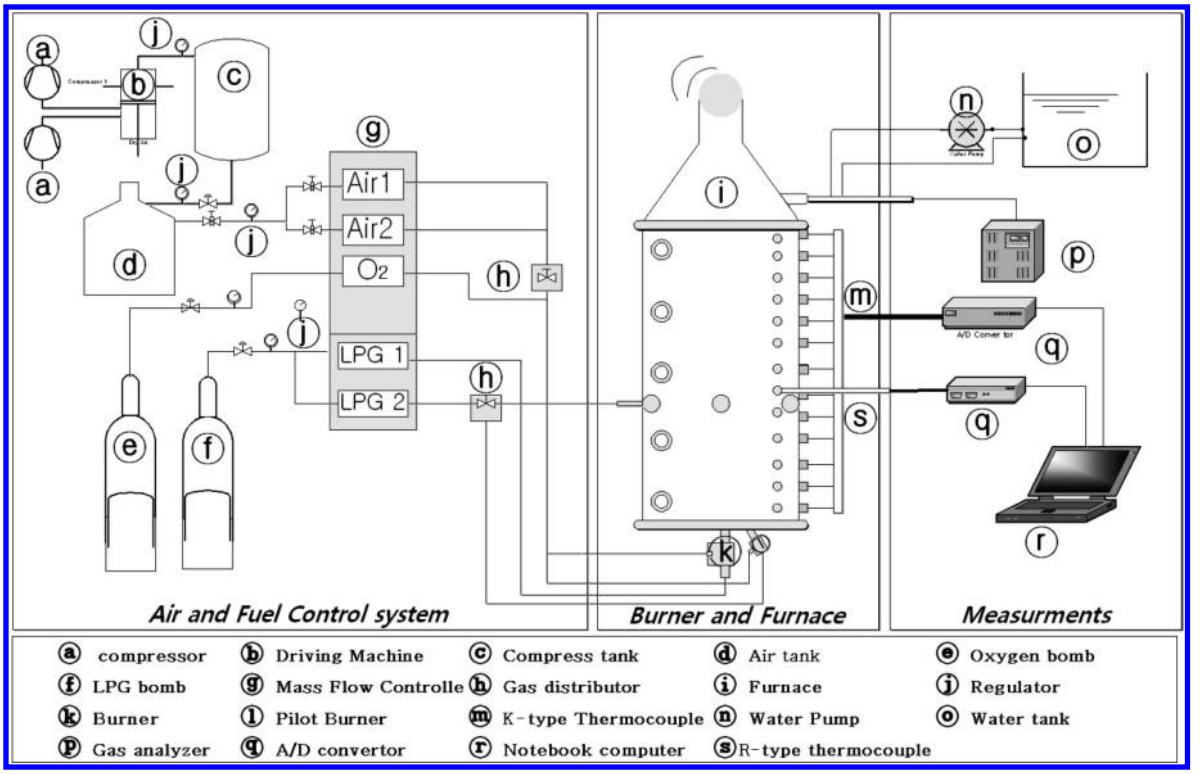

Figure 1. Schematic drawing of the experimental equipment.

paper to clarify the effect of internal flow field on the reburning process by using numerical analysis.

Numerical analysis of the NO_x formation and destruction process by the induced flow field and heat transfer characteristics in the combustion system can be used to investigate and improve understanding of the complex combustion mechanism. Therefore, a significant portion of this work focused on the numerical simulation of the NO_x generation and destruction process in various combustion circumstances. Zheng et al.[18] presented a numerical and experimental study on the reduction of NO_x emission in the furnace of a tangentially fired boiler under different operating conditions. An influence of the air/fuel ratio, combustion air temperature, and swirl angle on NO_x emission for a 160 MW industrial boiler was reported by Habib et al.[19] Determination of NO_x emissions from strong swirling confined flames within an integrated CFD-based procedure was reported by Frassoldati et al.[20] A numerical and experimental study was carried out by Kim et al.[21] in order to investigate the influence of the excess air ratio and tertiary air swirl number on the thermal and prompt NO production inside a 0.2 MW pilot-scale combustor.

In this paper, the results of experimental and numerical investigations on the effect of the fuel-lean reburning process on NO_x reduction in a lab-scale furnace are reported. To carry out experimental research, a vertically oriented 15 kW lab-scale furnace has been manufactured and fabricated. The experimental variables included the reburn fuel fraction and the location of the reburn fuel injection. In terms of numerical analysis, a computational fluid dynamics (CFD) model was used to predict the fluid flow and the heat transfer characteristics within the furnace under various operational conditions. Numerical analysis was conducted in a three-dimensional domain, including turbulence, chemical reaction, radiation, and NO modeling. The predicted numerical results were compared and validated with the available experimental data.

2. EXPERIMENTAL SECTION

A schematic of the experimental facility is shown in Figure 1. The experimental system was composed of a lab-scale furnace with a 15 kW burner as well as oxidizer/fuel supplying equipment and analyzing instruments for temperature and product gases. The combustion chamber, with an outer diameter of 0.5 m and a height of 1.2 m, was cylindrical and made of stainless steel. The ceramic fiber, Cerakwool, was installed along the inner furnace wall to prevent heat loss through the furnace's surface. The thickness of insulation was not greater than 0.04 m over the whole region. Therefore, the effective inner radius of the furnace was maintained at 0.21 m. At thirteen locations along the vertical direction of the furnace's outer region, the wall temperature was measured using K-type thermocouples in order to confirm the thermally steady state of the inner furnace region. When the wall temperature distribution did not change any more, it was determined that the inside furnace region had reached a thermally steady state condition. The gas temperature distribution of the inner furnace region was checked with R-type thermocouple. Regarding the K-type thermocouple, a variety of probes are available in the −200 °C to +1350 °C range. R-type thermocouples use a platinum−rhodium alloy containing 13% rhodium for one conductor and pure platinum for the other conductor so that they are usually used up to 1600 °C. The calibration of each thermocouple was carried out by using the proposed method mentioned in Baek et al.[22] Measured gas temperature was calibrated by using thermocouples with three different types of beads (0.3−0.5 mm). The local temperature at the same position was measured with thermocouples with different bead sizes. Then the results were extrapolated to the value at zero bead size.

Several reburn fuel injection ports (6 ports around the tangential direction for each layer and 7 locations in the axial direction) were designed to examine the effect of the reburn fuel injection location on

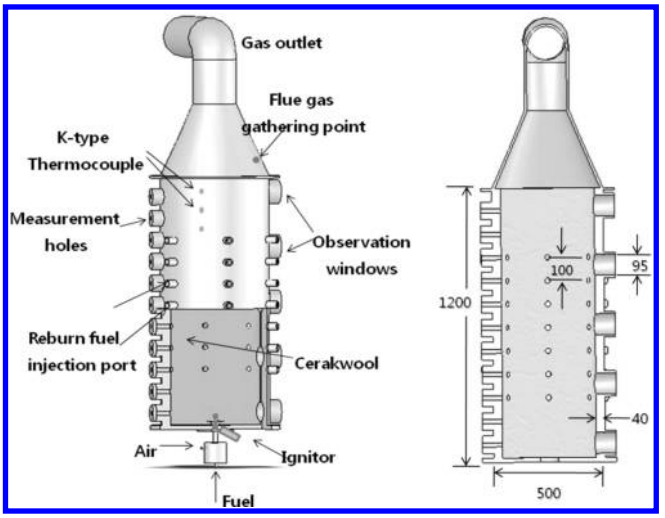

Figure 2. Detailed schematic of the lab-scale furnace.

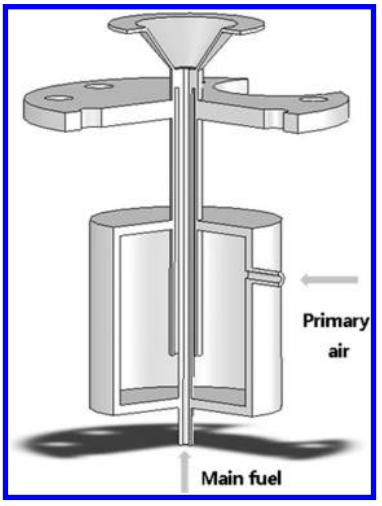

Figure 3. Detailed schematic of 15 kW burners.

the NO_x reduction for various experimental cases. A detailed schematic of the furnace is given in Figure 2. In most experimental cases, the amount of reburn fuel fraction has been limited to 13% of total heat input due to the increasing use of an oxidizer in the main combustion zone.

For injecting reburn fuel, a flat type nozzle with spray angles of 95° was used. The diameter of each nozzlewas 0.66 mm. The flow rate of injected reburn fuel was controlled by using a mass flow controlled. The injection velocity of reburn fuel was varied between 3.5 and 12.5 m/s according to the reburn fuel fraction.

The fuel and oxidizer gas stream inlet velocities were controlled to have a similar value (12−13 m/sec). The flow rate of oxidizer and fuel was 5.6×10^{-3} and 3.06×10^{-4} kg/s, respectively, in the case of stoichiometric combustion.

The gas analyzer (GreenLine MK2) was used to analyze the product gas for CO, O_2, NO, and NO_2. Product gases were taken from the stack of the furnace, located 1.2 m away from the burner tip, by using a water-cooled stainless steel probe. The error limit of O_2 concentration was estimated to be ±0.1% (vol.), and in terms of the other species (CO, NO and NO_2) the error limits were not more than ±0.1 ppm.

The configuration of the LPG diffusion flame burner, shown in Figure 3, consisted of a 4-mm inner pipe for fuel. The mass flow rates of the main fuel, oxidizer, and reburn fuel were periodically calibrated by a wet gas meter (Shinagawa, W-NK-10).

Table 1. Experimental Parameters

operating parameter	value
thermal input (kW)	
primary fuel	15
reburn fuel	0−2.25
(reburn fuel fraction)	(0−0.13)
injection velocity (m/sec)	
primary fuel (@300 K)	12.8
oxidizer (@300 K)	12.7
reburn fuel (@300 K)	0−12.5
equivalence ratio (φ) of primary zone	0.79
equivalence ratio (φ) of reburning zone	0.84−0.98
reburn zone location (from burner tip, m)	0.3−0.7

For flame stabilization, the burners were equipped with a vane swirler in order to generate a swirl-induced recirculation zone. In this study, the swirler vane angle is fixed at 45°. The swirl number is defined as follows:[23]

$$S = \frac{2}{3}\left[\frac{1-(D_h/D)^3}{1-(D_h/D)^2}\right]\tan\theta \quad (1)$$

where D is the inner diameter of the swirler, D_h is the hub diameter of the swirler, and θ is the swirler vane angle. Therefore, the swirl number is set to 0.76. The burner is also outfitted with a quarl section in order to improve flame stabilization.

As LPG, which consists of 95% of propane and 5% of other mixtures such as butane and methane, etc., was used as the main and reburn fuel in this study, the amount of main fuel was always fixed to maintain the thermal input condition of the primary zone.

The distance of reburning zone wa defined as the distance from the reburn fuel injection point of the furnace to the extraction point for product gases (1.2 m away from the burner tip). The efficiency of NO_x reduction depends on the varying amount of reburn fuel. In this case, the reburn fuel fraction was varied from 0 to 0.13 of the total heat input. The reburn fuel fraction, rff, here is defined by[24]

$$\text{rff} = \frac{\text{the amount of the reburn fuel}}{\text{the amount of the main fuel} + \text{the amount of the reburn fuel}} \quad (2)$$

Table 1 indicates the overall operating conditions for experiments.

3. MODELING ANALYSIS PROCEDURE

The numerical simulation of the 15 kW laboratory-scale furnace was conducted on a three-dimensional domain in order to examine flow pattern, as well as thermal and pollution characteristics of the reacting flows. The operating parameters include the reburn fuel fraction and the location of the reburn fuel injection. A nonuniform unstructured mesh composed of 345,000 cells was used. A fine discretization was used at inlet region as well as at the reburn fuel injection point to give high resolution when required. A test with finer grid (less than 250,000 and up to 450,000 cells) proved that the current grid system sufficiently provides grid independent solutions.

3.1. Governing Equation. Numerical calculations were carried out using a commercial computational code (FLUENT 6.3 version) while a three-dimensional furnace geometry was created by GAMBIT 2.4. The equations that govern the conservation of mass, momentum, and energy, as well as the equation of species

transport, can be expressed in the following general form:

$$\frac{\partial}{\partial t}(\rho \cdot \Phi) + \frac{\partial}{\partial x_i}(\rho \cdot u_i \cdot \Phi) = \frac{\partial}{\partial x_i}\left(\Gamma_\Phi \cdot \frac{\partial \Phi}{\partial x_i}\right) + S_\Phi \quad (3)$$

where Φ represents the dependent variable and u_i is the velocity component along the coordinate direction x_i; ρ expresses the fluid density; Γ_Φ is the diffusion coefficient; and S_Φ is the source or sink term.

Equation 3 stands for the continuity equation when $\Phi = 1$, while a substitution of velocity components into Φ generates the momentum equation for each respective direction. The conservation equation for the species mass fraction and the enthalpy can be obtained when the mass fraction Y_i or the mixture enthalpy, h, is substituted into Φ.

The realizable k-ε model and the standard k-ε model, which solves transport equation for kinetic energy (k) and its dissipation rate (ε), are used for flow prediction in this study. To predict the temperature distributions inside the furnace, the discrete ordinate method (DOM) radiation model is considered. The DOM model solves the radiative heat transfer equation for a finite number of discrete solid angles. The model is applicable over a wide optical thickness range and accounts for the scattering of radiant heat from solid particles. Absorption coefficients of the gas phase are calculated by using the weighted-sum-of-gray-gases model (WSGGM).[25]

As the analysis deals with nonpremixed turbulent flames, a suitable scheme is required for coupling the turbulent mixing and the reactions of major species. In the current experimental case, the primary combustion consists of a diffusion flame (nonpremixed combustion). In these flames, it can generally be assumed that the turbulent mixing rate is much slower than the chemical kinetics rates (fast chemistry). The current study uses the eddy-dissipation combustion model assuming that the reaction rate is controlled by the turbulent mixing rate. Hence, the turbulent mixing rate in conjunction with a global reaction mechanism is used to predict local temperatures and species profiles. This model solves the conservation equations describing convection, diffusion, and reaction sources for each component species.[23] Detailed formulations of the models can be found in the FLUENT 6.3 manual.[27]

3.2. NO modeling. The NO_x formation and destruction processes in combustion systems are very complex phenomenon. During the combustion reaction, nitrogen either in the air or in the fuel is converted to nitrogen-containing pollutants such as NO, NO_2, N_2O, NH_3, and HCN. The pollutant species formed depends on the temperature and fuel/oxygen ratio in the combustion zone.[3−5,26] The processes for formation and depletion of nitrogen oxides are highly complex, involving a large number of intermediate species. However, in this study, only a few global steps are considered for simulating NO_x formation to facilitate their interaction with velocity, temperature, and concentration field.

The chemical reactions involved in the NO formation may be decoupled from the other species, since the amount of NO formed is small (and therefore does not affect the overall heat or mass balances) and NO formation by the thermal mechanism is generally slow compared to the fuel oxidation. Therefore, the NO concentration is postcalculated after the velocity, temperature, turbulence, and major species concentration are obtained. The mass transport equation for the NO species is solved by taking into account the convection, diffusion, production, and consumption of NO and related species. Thermal NO_x, prompt NO_x, and fuel NO_x formations pathways are the most important chemical kinetic processes during combustion. However, the fuel NO_x chemical kinetics can be neglected in this calculation, since LPG contains a negligible amount of nitrogen.

Thermal NO_x is formed by the oxidation of atmospheric nitrogen present in the combustion air. The formation of thermal NO_x is strongly affected by the temperature-dependent chemical reactions known as the extended Zeldovich mechanism.[28]

For thermal and prompt NO, the NO species transport equation is given by

$$\frac{\partial}{\partial t}(\rho \cdot Y_{NO}) + \frac{\partial}{\partial x_i} \cdot (\rho \cdot u_i \cdot Y_{NO}) = \frac{\partial}{\partial x_i}\left(\Gamma_\Phi \cdot \frac{\partial Y_{NO}}{\partial x_i}\right) + S_{NO} \quad (4)$$

where the Y_{NO} is the mass fraction of NO in the gas phase and S_{NO} indicates source term for different NO_x mechanism. Using the NO transport eq 4, the net rate of the formation of NO through the extended Zeldovich mechanism is given by

$$d[NO]/dt = k_{f,1}[O][N_2] + k_{f,2}[N][O_2] + k_{f,3}[N][OH] - k_{r,1}[NO][N] - k_{r,2}[NO][O] - k_{r,3}[NO][H] \quad (5)$$

where all concentrations have units of gmol/m^3. In the above expressions $k_{f1,2,3}$ and $k_{r1,2,3}$ are the kinetic rate constants for each of the forward and reverse reactions R3−R4. The data of the kinetic rate constants are determined from using the evaluation of Hanson and Salimain.[29]

During the combustion of hydrocarbon fuel, the NO_x formation rate exceeds the expected amount of NO_x that originates from the reaction of thermal NO_x. This is prompt NO_x which was first identified by Fenimore.[30] Prompt NO_x is generated from the rapid reaction of atmospheric nitrogen with hydrocarbon radicals. Prompt NO_x is generally minor compared to the overall quantity of fuel or thermal NO_x generated from combustion. However, as NO_x emissions are reduced to extremely low limits, the contribution of this source becomes more important. The reaction mechanism for the prompt NO formation is given below.

$$CH + N_2 \leftrightarrow HCN + N \quad (R3)$$

$$CH_2 + N_2 \leftrightarrow HCN + NH \quad (R4)$$

$$N + O_2 \leftrightarrow NO + O \quad (R5)$$

$$HCN + OH \leftrightarrow CN + H_2O \quad (R6)$$

$$CN + O_2 \leftrightarrow NO + CO \quad (R7)$$

CH and CH_2 generated from hydrocarbon fuel fragmentation play an important role as the source of prompt NO_x in combustion. Products (NH or N) in reactions (R3−R4) are expected to finally bring more NO_x generation through formation of amine and cyano compounds. It is well-known that amine and cyano compounds are the important intermediate species in fuel NO_x generation. In the present NO model, an assumed shape of probability density function (Beta PDF) in terms of normalized temperature and oxygen species mass fraction is used to predict

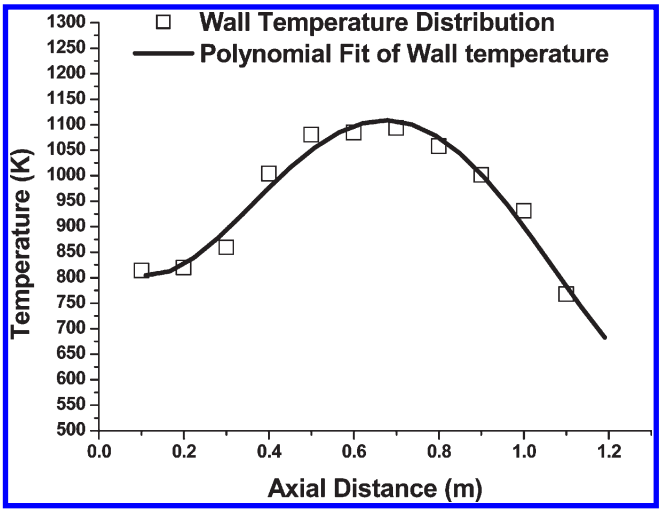

Figure 4. Temperature distributions on the inner wall of the furnace along the axial direction (at φ = 0.91, without reburning).

the NO emission in turbulent flows to account for the temperature and composition fluctuations.

3.3. Reburning. The reburning process is used to reduce NO emissions by adding a hydrocarbon fuel downstream of the combustion zone. When the reburn fuel is injected into the reburning zone, a fuel-rich zone is locally created at the specific region. However, an overall fuel-lean condition is still maintained from the viewpoint of the whole furnace region, based on the ratio of the total amount of fuel mass to the total amount of air. A partially fuel-rich zone then provides CH_i radicals to react with any available NO to form HCN. The following equations are considered to be the most important reactions of NO reduction by CH radicals. The forward rate is found to be dominant[8]

$$NO + CH_2 \rightarrow HCN + OH \quad (R8)$$

$$NO + CH \rightarrow HCN + O \quad (R9)$$

$$NO + C \rightarrow CN + O \quad (R10)$$

There are two types of available models to describe the kinetics of NO_x destruction in the reburn zone. In this study, the partial equilibrium approach is used, based on the model reported by Kandamby et al.[31] and Su et al.[32] The partial equilibrium is used to calculate important reactant species of reburning process such as CH_i, HCN, and NO. The partial equilibrium approach adds a reduction path to De Soete's global model. In this model, two additional chemical pathways are introduced; NO + $CH_i \rightarrow$ HCN and NO + $CH_i \rightarrow$ products. These additional chemical reactions account for the NO destruction in the reburning zone.

3.4. Numerical Investigation. The steady state simulations are performed by using the commercial CFD code FLUENT 6.3, which is based on the finite-volume method. The SIMPLE algorithm is used to interpret the pressure interpolation and the coupling of pressure and velocity, respectively. A criterion for convergence is used so that the solution is considered to be convergent when the maximum of the residuals of the continuity and turbulence of each velocity components of control volumes are less than 10^{-3}, while for the radiation and energy equation they are less than 10^{-6}. It is clear that accurate boundary conditions are essential for predicting accurate numerical results.

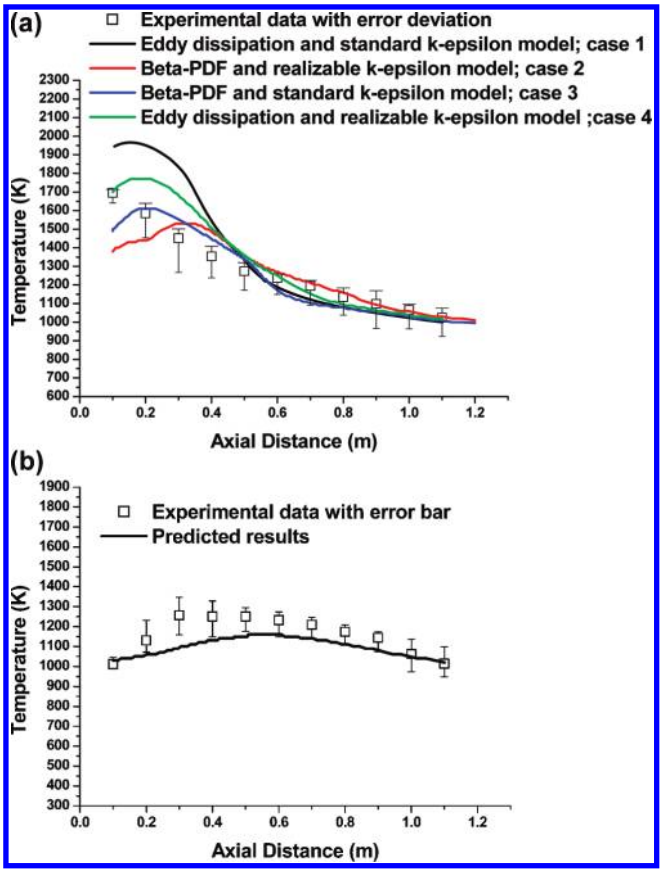

Figure 5. (a) Comparison of temperature distribution using different combustion and turbulence models along the furnace centerline (at φ = 0.91, without reburning). (b) Comparison of calculated and measured temperature distributions along the furnace 0.1 m apart from the centerline in a radial direction (at φ = 0.91, without reburning).

Especially, the measured temperature distribution on the furnace's outer region is used to represent the temperature boundary condition as shown in Figure 4.

4. RESULTS AND DISCUSSION

4.1. Validation of the Numerical Results. Numerical prediction provided by CFD calculations are validated against experimental results. The temperature, CO, and NO_x concentration along the furnace centerline are compared with experimental data without any reburning process for the equivalence ratio, φ = 0.91. The comparisons of the calculated and measured data are shown in Figure 5a,b and 6a,b. For the validation of temperature distribution, two locations such as the centerline and an axial direction at 0.1 m away from the axis of symmetry are selected to compare the numerical and experimental results. The measured temperature is collected by an A/D convertor (IO tech, Personal Daq/56) which operates at 7.5 Hz. The temperature continues to be measured until 100 samples of temperature are gathered. After that, the average temperature value is taken from dividing all the temperatures added together by the total sample number. The average of the temperature sample data and the error deviation are presented together in the final results. The value of deviation of temperature distribution consists of the maximum temperature minus the average temperature and the average temperature minus the minimum temperature. As shown in Figure 5a and b,

dx.doi.org/10.1021/ef101386h |*Energy Fuels* 2011, 25, 905–915

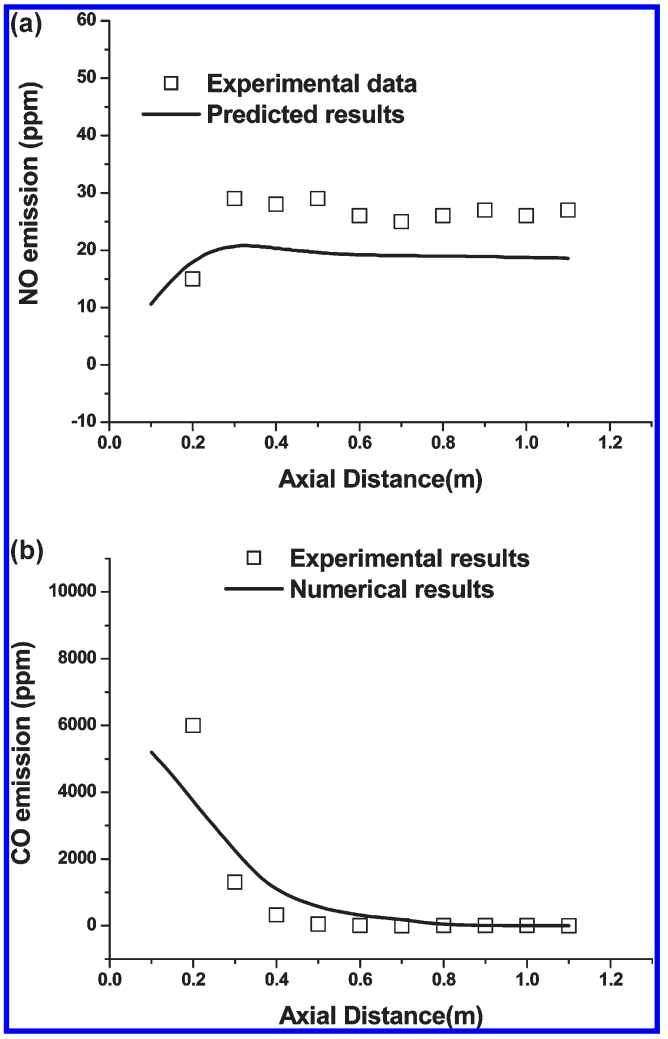

Figure 6. (a) Comparison of calculated and measured distributions of NO emission along the furnace centerline (at $\varphi = 0.91$, without reburning). (b) Comparison of calculated and measured distribution of CO emission along the furnace centerline (at $\varphi = 0.91$, without reburning).

the predicted temperature distribution matches well with the measured data, although a small difference is observed in the flame development region (0−0.4 m) which is close to the bottom of the furnace. Especially, in Figure 5a, four cases of different turbulence and combustion models are considered to determine the effect of the turbulence or the combustion model on the predicted results. Among others in Figure 5a, the results for case 4 with eddy dissipation combustion and realizable k-ε turbulence models are observed to be much better that those for case 1 with eddy dissipation combustion and standard k-ε model. The cases 2 and 3 with β-function PDF combustion model produces relatively low temperature distributions near the flame development region (0−0.4 m). In addition, the β-function PDF combustion model does not sufficiently predict the NO_x emission level, which yields only limited value of less than 0.1 ppm. The goal of this paper is to find out the effect of the fuel-lean reburning process on NO_x reduction in a combustion environment. Therefore, it is important to predict the NO_x emission level with good accuracy. In this respect, the case 4 with the eddy dissipation combustion and realizable k-ε turbulence models is considered to be most appropriate.

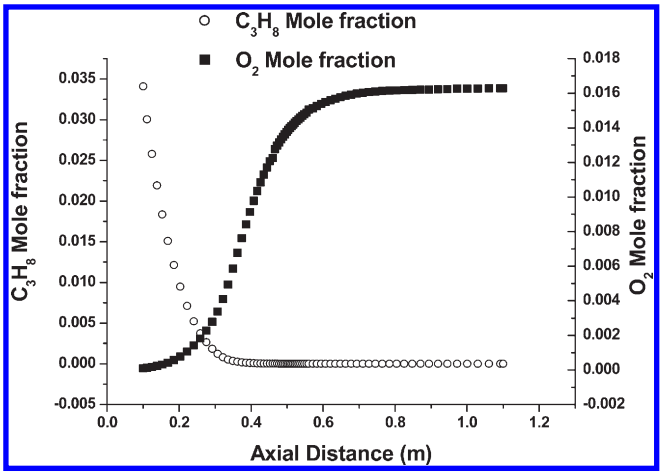

Figure 7. Predicted results of propane (C_3H_8) and oxygen (O_2) mole fraction along the axial direction (at $\varphi = 0.91$, without reburning).

The reason for this discrepancy could be explained by numerical and experimental errors. Several experimental errors such as thermocouple, A/D convertor, and other measuring equipment, even if calibrated, may also have caused the small difference between the numerical and experimental results. These experimental errors sometimes account for a larger part of the observed difference. In spite of that, the comparison between the measured and calculated results shows a good agreement.

The results of the validated temperature distribution indicate that the calculated results well describe the flow field and heat transfer, because the overall temperature distribution of the inlet furnace region is not only dependent on the heat transfer rate but also on the flow field induced by the primary combustion reaction. Therefore, the realizable k-ε turbulence model could be considered well-adapted enough to conduct the present numerical approach.

Figure 6a and b show the comparisons between the predicted and measured NO and CO concentrations along the furnace centerline, respectively. The predicted results of the NO and CO concentration show overall good agreement with the measured data. Figure 6a shows that the amount of NO emission level increases up to 0.3−0.4 m from the burner tip. As shown in Figure 6b, CO emission sharply increases in the near flame generation region (0−0.3 m at the axial direction in the centerline), because the supplied main fuel does not completely react with oxidizer due to a local lack of oxidizer in the main combustion zone in which the oxidizer spreads out in a radial direction due to the influence of a swirler. Afterward, along the downstream CO emitted therein rapidly decreases while reacting with affluent oxygen.

The predicted results of propane (C_3H_8) and oxygen (O_2) mole fraction along the axial direction, as shown in Figure 7, illustrate that the flame induced by the primary combustion reaction is usually observed up to 0−0.3 and 0.4 m away from the burner tip. The propane is mostly consumed up to 0.4 m from the burner tip, while the oxygen (O_2) mole fraction dramatically increases after 0.3 m from the burner tip, reaching its steady state above 0.6 m. These trends show that the combustion reaction mainly occurs in the range of 0−0.4 m along the axial direction, while mixing process between reburn fuel and oxidizer is extended up to 0.6−0.7 m from the burner tip. These results indicate that nonuniformities are generated in the internal flow region inside the furnace.

dx.doi.org/10.1021/ef101386h |*Energy Fuels* 2011, 25, 905–915

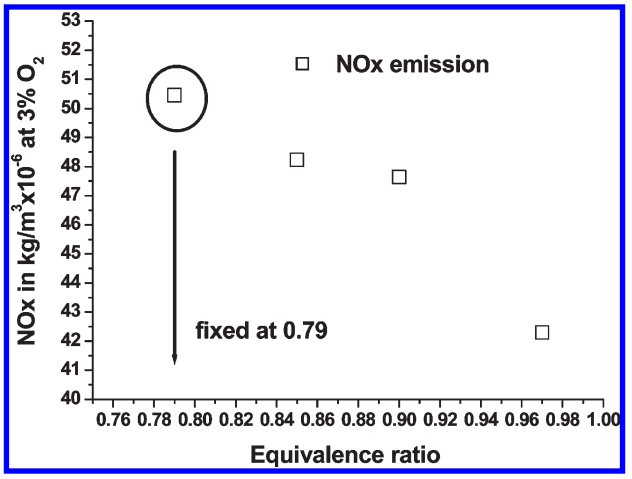

Figure 8. NO_x emission according to the equivalence ratio in the primary combustion zone.

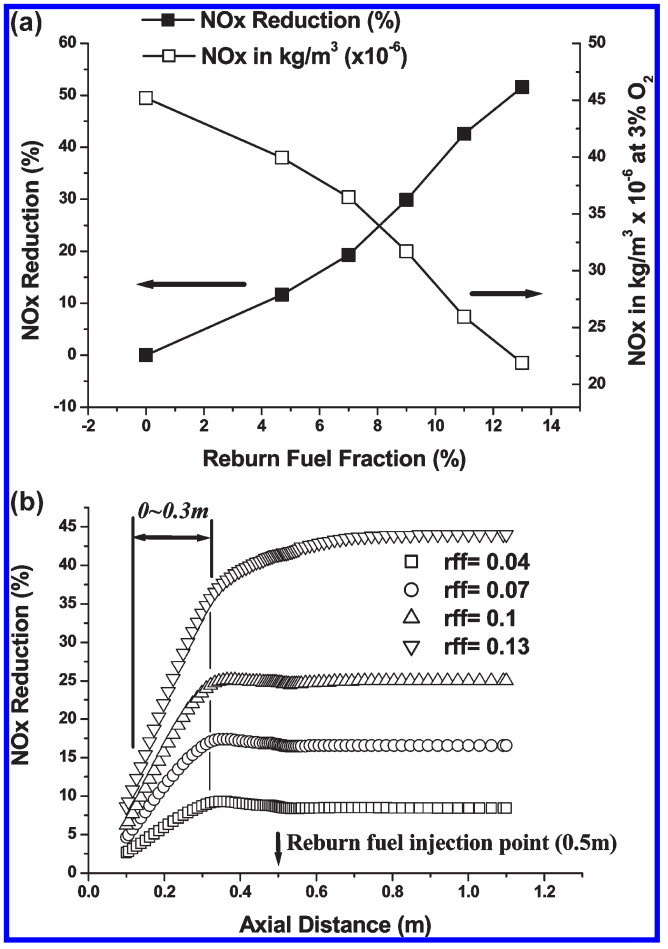

Figure 9. (a) Effect of reburn fuel fraction on NO_x reduction and emission (at 3% O_2 dry basis) (measured data). (b) Predicted results of NO_x reduction for different reburn fuel fractions along the axial direction of the furnace centerline.

Through the above validation procedure, the numerical methods used in this study prove that this method can predict the combustion characteristics, heat transfer, and flow field of a laboratory--scale furnace.

4.2. NO_x Reduction. In the following section, the effectiveness of the fuel-lean reburning system on reduction of emissions of NO_x and CO is verified through several experiments. Numerical simulation also provides deep insight into the effectiveness of the thermo-fluid dynamic field on the reburning process. All experimental cases are conducted and measured in a thermally steady state condition by preheating the furnace.

The amount of oxidizer is an important factor affecting the NO_x emission from the primary combustion zone. Figure 8 shows the NO_x production from LPG diffusion flame as a function of the equivalence ratio in the primary combustion zone without the reburning process. Increasing the oxidizer in the primary combustion zone (decreasing equivalence ratio) favors the formation of NO_x species, since the concentration of NO_x in the flue gas can be proportional to that of the nitrogen compound in the primary combustion zone. In this study, equivalence ratio in the primary combustion zone is fixed at 0.79 to maintain NO_x production without reburning process.

The method used to evaluate the effect of various reburn fuel fractions on NO_x reduction is also conducted by using the fuel-lean reburning method. Reburn fuel fraction is varied between 0 and 0.13 of total heat input and it is injected 0.5 m away from the burner tip. Based on this, NO_x reduction is represented for different reburn fuel fractions in Figure 9a, in which NO_x concentration is represented in kg/m^3 ($\times 10^{-6}$) of dry gas based on 3% of O_2 concentration. The NO_x reduction steadily increases as the reburn fuel fraction reaches about 0.13. As stated in the above section, under locally fuel-rich conditions, the following kinetics pathways control the efficiency of reburning:[3−5]

$$C, CH, CH_2 + NO \rightarrow HCN + \ldots \quad (R11)$$

$$HCN + O \rightarrow NCO + H \quad (R12)$$

$$NCO + H \rightarrow NH + CO \quad (R13)$$

$$NH + H \rightarrow N + H_2 \quad (R14)$$

$$N + NO \rightarrow N_2 + O \quad (R15)$$

As shown in reaction R11, the partial oxidation and pyrolysis of the injected hydrocarbon fuel results in the formation of CH_i radicals. These radicals react with NO, thereby generating HCN radicals, which are known as the intermediate species that can initiate NO_x removal reactions in the reburning zone. HCN radicals undergo several reactions, and then eventually, nitrogen oxides change into nitrogen molecules. The formation of HCN radicals generally depends on the concentration of hydrocarbon radicals. Therefore, increasing the amount of reburn fuel can lead to a higher reduction of nitrogen oxides by increasing the injected reburn fuel.

Using this laboratory furnace, the maximum NO_x reduction value is observed to be 50% (at 3% O_2 dry basis), when the reburn fuel fraction reaches 0.13. In this study, the reburn fuel fraction is limited to 0.13 due to the increase in the amount of oxidizer. When the reburn fuel fraction reaches 0.13, the equivalence ratio of the primary zone has to be maintained about 0.79 in order to maintain the overall fuel-lean condition in the whole furnace region including the reburning zone.

Figure 9b indicates the results of numerical prediction of the above experiments. As previously mentioned, rff represents the

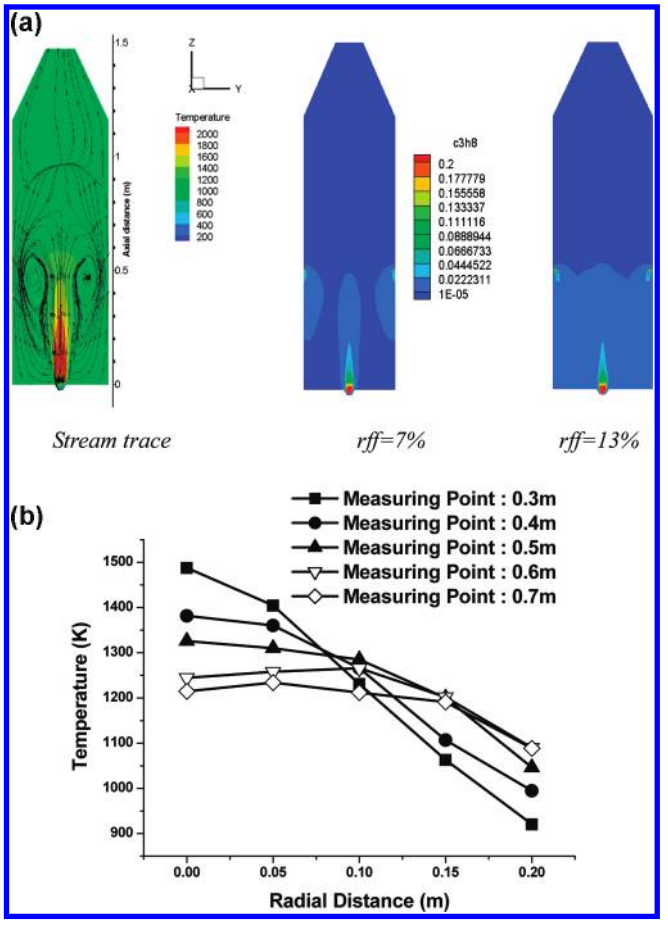

Figure 10. (a) Predicted stream trace and C_3H_8 mole fraction contour for two reburn fuel fractions. (b) Radial temperature distribution for different axial measuring positions (at φ = 0.79, rff = 0.13).

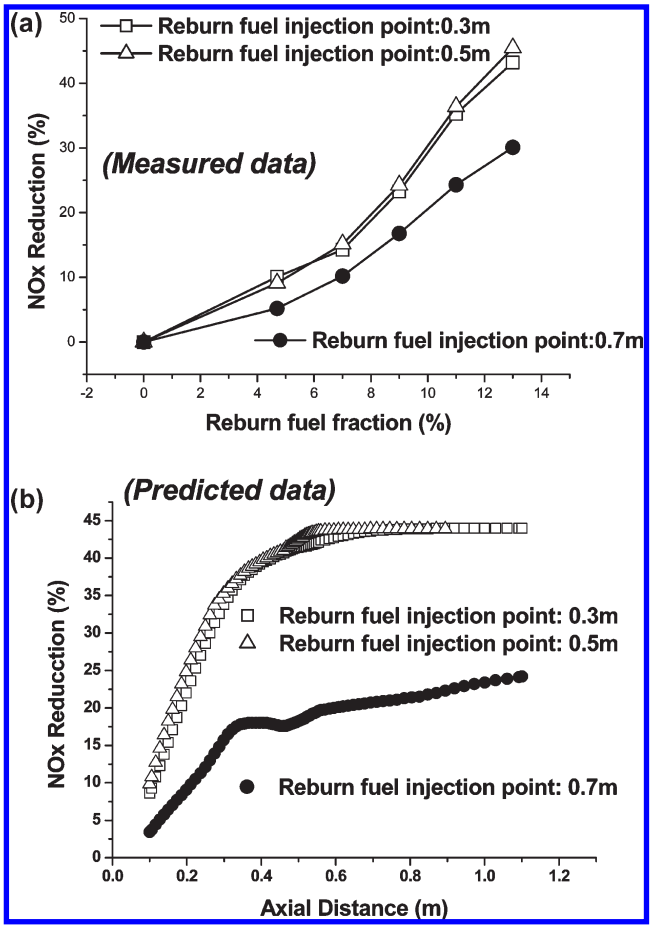

Figure 11. (a) Effect of reburn fuel fraction on NO_x reduction for different locations of reburn fuel injection. (b) Predicted results of NO_x reduction for different locations of reburn fuel injection with 0.13 reburn fuel fraction.

reburn fuel fraction. The predicted result of NO_x reduction for different reburn fuel fractions along the axial direction of the furnace centerline is shown in Figure 9b, which shows that the predicted results fit well with the measured data. The predicted NO_x reduction also achieves about 50% with the reburn fuel fraction of 0.13. However, most of the NO_x destruction reactions occur in the further upstream region (0−0.3 m), although the location of injected reburn fuel is 0.5 m away from the burner tip, as shown in Figure 9b. The reason for this phenomenon can be explained by the fact that the flow stream of the injected reburn fuel interferes with the recirculation flow induced by the primary combustion in the furnace. Therefore, the injected reburn fuel may be drawn into the upstream region of the furnace, instead of remaining in the injected region. The mole fraction contours of fuel (C_3H_8) for different reburn fuel fraction conditions and the stream trace for the main flow of primary combustion zone in Figure 10a show clearly the effect of the inner main flow stream on the injected reburn fuel. As shown in the stream trace in Figure 10a, the inner flow field is divided into two major flows; downstream and recirculation flow.

This recirculation flow could also be verified by the radial temperature distribution as shown in Figure 10b. In the case of the upstream region of the furnace (measuring point ≤0.5 m), the radial temperature distribution rapidly changes due to the recirculation flow, when the measured point moves toward the wall from the center of the furnace. However, in the downstream region (measuring point ≥0.6 m) the radial temperature is more uniform. These results support the predicted results in Figure 10.

Figure 11a and b show the experimental and numerical results for the effect of reburn fuel injection location on NO_x reduction. Based on this comparison it is observed that the location of reburn fuel injection has to be carefully selected in order to achieve the desired NO_x reduction. NO_x reduction reaches 50% with a 0.13 reburn fuel fraction, when the location of the reburn fuel injection is 0.3 and 0.5 m from the burner tip. In this range, the injected reburn fuel has more residence time and blends well with the flue gases by interacting with the recirculation flow. Therefore, a higher NO_x reduction could be achieved. However, at the location of the reburn fuel injection of 0.7 m, NO_x reduction is below 30% in spite of a 0.13 reburn fuel fraction of total heat input.

Figure 12 shows the predicted results of O_2 mole fraction under the reburning process. As the reburn fuel fraction increases, O_2 mole fraction in the product gas is observed to decrease. When the location of the reburn fuel injection is 0.5 m from the burner tip at port 3, most of the O_2 is consumed by reaction with the injected reburn fuel in the upstream region of the furnace (0−0.5 m) due to the recirculation flow. On the other hand, the reburning process occurs in the downstream region (0.6−1.0 m) when the reburn fuel is injected from port 5 at 0.7 m from the burner tip.

dx.doi.org/10.1021/ef101386h |*Energy Fuels* 2011, 25, 905–915

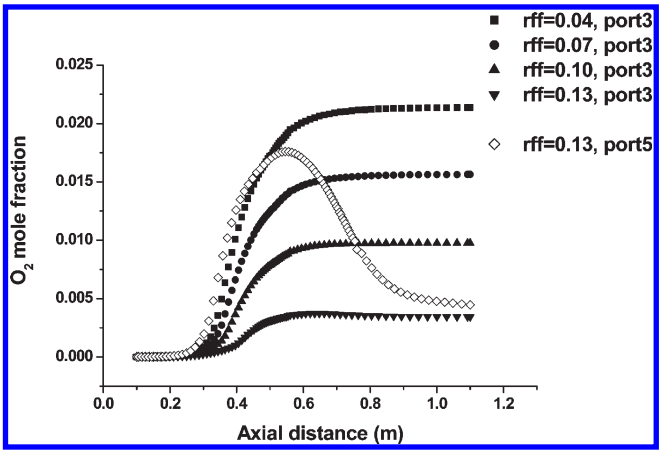

Figure 12. Predicted results of O_2 mole fraction for different locations of reburn fuel injection for various reburn fuel fractions.

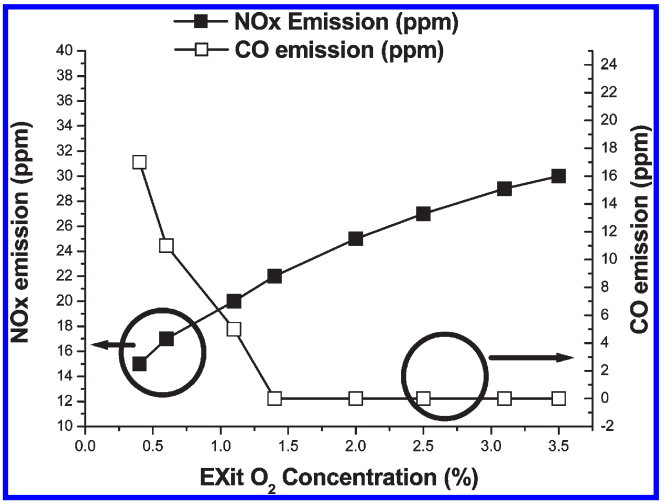

Figure 13. NO_x and CO emission according to the exit O_2 concentration (measured data) (at φ = 0.91, rff = 0.18).

As previously mentioned, introducing additional air could generate unexpected problems when the conventional reburning process is used to reduce NO_x. To verify this phenomenon, the following experiment is carried out. The initial O_2 concentration and reburn fuel fraction are fixed at 3.0% and 0.18, respectively, to make a fuel-rich condition in the reburning zone. The distance between the reburning zone and burnout zone is fixed at 0.4 m. Initial O_2 concentration represents the O_2 concentration in the product gas before reburning. Then the exit O_2 concentration, which means the O_2 concentration in the product gas after reburning, depends on the amount of additional air. As shown in Figure 13, a decrease in exit O_2 concentration results in less NO_x emission in the product gas. In other words, a decrease in the amount of additional air can achieve more NO_x reduction.

When the injected reburn fuel is fully consumed, a small fraction of the HCN intermediate remains and then this radical reacts with OH, thereby providing another source term for NO_x. Consequently, the method of the conventional reburning process possibly can generate more NO_x emission compared with the fuel-lean reburning system.

4.3. CO Emission. The limited CO generation from the furnace is critical in the industrial facilities when the fuel-lean

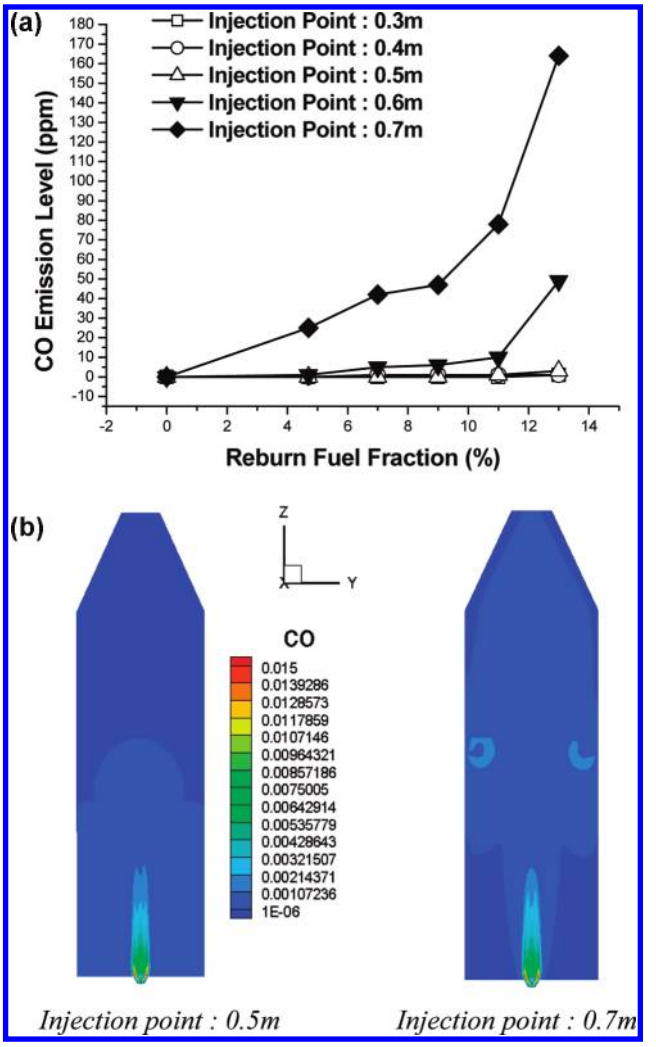

Figure 14. (a) Effect of reburn fuel fraction on CO emission for different injection points (measured data). (b) Predicted results of CO mole fraction contour for different reburn fuel injection points.

reburning system is used as the De-NO_x method, since additional air is not used anymore to burn the remaining CO as well as unreacted hydrocarbon radicals. It is well-known that the reaction of CO oxidation is strongly dependent on the equivalence ratio and temperature distribution. OH is one of the most important radicals for combustion at a high temperature region, and its oxidation reaction role with CO is known to be[33]

$$CO + OH \rightarrow CO_2 + H \qquad (R16)$$

Previous studies have shown that the CO oxidation reaction usually takes place in a temperature region higher than 1300 K in the fuel-lean reburning technique to reduce NO_x. It is also known that the CO emission characteristics in various reburning processes are dependent upon the optimal reburn fuel injection point in a fuel-lean reburning system. Therefore, in this study the locations of reburn fuel injection as well as the amount of reburn fuel are selected as parameters to influence CO emission. There is only a minor change in CO emissions when the reburn fuel injection is located between 0.3 and 0.5 m as shown in Figure 14a. However, when it increases further, the CO emission reaches a maximum of 175 ppm (at 3% O_2 dry basis) for the reburn fuel fraction of 0.13 at an injection point of 0.7 m away from the

dx.doi.org/10.1021/ef101386h |*Energy Fuels* 2011, 25, 905–915

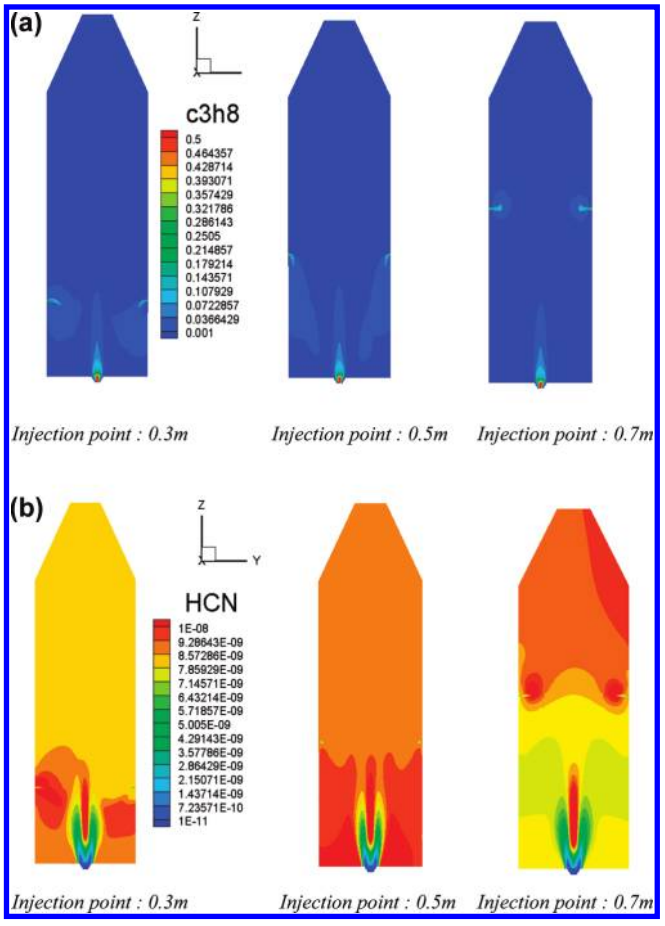

Figure 15. (a) Predicted results of propane (C_3H_8) mole fraction contour with different reburn fuel injection points. (b) Predicted results of HCN mole fraction contour for different reburn fuel injection points.

burner tip. Predicted results of CO mole fraction in Figure 14b further support this observation

Meanwhile, Figure 10b indicates that the temperature between 0.1 and 0.2 m in a radial direction, when the reburn fuel injection point is below 0.5 m from the burner tip, does not reach 1300 K. On the contrary, the other regions (0−0.1 m in radial direction) are maintained at a higher temperature than 1300 K which is quite high enough to limit CO generation, as previously stated in Hura and Breen.[15]

The characteristic of CO emission can be explained by the predicted results of Figure 15a and b. At the reburn fuel injection point (0.3−0.5 m) where CO emission is negligible, injected reburn fuel experiences temperatures lower than 1300 K as shown in Figure 10b. However, it is shortly entrained into a region with temperature higher than 1300 K by flowing into the upstream region due to the recirculation flow. In contrast, for the case of sharply increasing CO emission (injection point 0.6−0.7 m), the injected reburn fuel is not entrained into the upstream region since the effect of recirculation flow is not available in this region. As a result, the distribution of the HCN radicals, which are formed by the reburning process, is also observed to be different according to the reburn fuel injection point as shown in Figure 15b, as expected.

As the experimental and numerical results show above, the recirculation flow of the flue gas strongly affects the NO_x reduction and CO emission of the fuel lean reburning process by disturbing the reburn fuel stream.

5. CONCLUSIONS

The effectiveness of the fuel lean reburning process for reducing NO_x and the influence of recirculation flow of flue gases on the reburning process were experimentally as well as numerically evaluated in a lab-scale furnace by changing the reburn fuel fraction, the location of the reburn fuel injection, and the inlet velocity of the oxidizer. The results obtained have provided useful information for the control of fuel-lean reburning process and a better knowledge of the key parameters needed for NO_x reduction efficiency and limiting CO emission. For the experiments, a 15 kW lab-scale furnace was designed and fabricated and LPG was used as the main and reburn fuel. Numerical simulation was also conducted on a three-dimension domain to provide predictions of the flow pattern, as well as thermal and pollutant characteristics of reacting flows by using comprehensive models for the combustion process and NO_x generation and destruction. The results are summarized as follows:

(1) Predicted results provided by CFD calculations have been validated against the experimental results. The temperature distribution, as well as CO and NO_x concentration along the furnace centerline, was compared with experimental data without any reburning process for the given experimental condition. Through the comparison between the experimental results and calculated data, the numerical methods used proved that they were well adapted for predicting virtual combustion circumstances.

(2) The fuel-lean reburning process could attain up to 50% NO_x reduction (at 3% O_2 dry basis) with a reburn fuel fraction of just 0.13. The CO emission was found to be significantly dependent on the location of the reburn fuel injection, as well as the amount of injected reburn fuel, as shown in related experimental studies.

(3) Several predicted results provided insight and understanding about how the recirculation flow induced by the primary combustion affected the reburning process. As presented in the above experimental and numerical results, the recirculation flow was predominant in the range of 0−0.5 m from the burner tip. Therefore, in this range, the injected reburn fuel had a longer residence time and blended well with flue gases, since it was injected into the upstream region of the furnace. For this reason, the role of the recirculation flow had to be carefully understood in order to enhance the NO_x reduction and to limit CO emissions.

(4) This paper showed that the fuel lean reburning process is a more attractive way compared with the conventional reburning process to reduce NO_x emission. In the case of the conventional reburning process, remaining HCN radicals in the reburning zone reacted with OH, thereby adding another NO_x source term. The amount of additional air was represented in the exit O_2 concentration. A decrease in exit O_2 concentration resulted in less NO_x emission in the product gas.

AUTHOR INFORMATION

Corresponding Author

*Tel.: (82-42) 869-3714; fax: (82-42) 869-3710; e-mail: swbaek@kaist.ac.kr.

ACKNOWLEDGMENT

This work was supported by the "Human Resources Development" of the Korea Institute of Energy Technology Evaluation and Planning (KETEP) grant funded by the Korea government Ministry of Knowledge Economy.

NOMENCLATURE

S = swirl number
θ = van angle
D = nozzle diameter
D_h = van hub diameter
rff = reburn fuel fraction
Φ = dependent variable
u_j = velocity component
φ = equivalence ratio
x_j = coordinate direction
P = fluid density
Γ_Φ = diffusion coefficient
S_Φ = source or sink term
Y_i = species mass fraction
h = mixture enthalpy
$k_{f1,2,3}$ = forward kinetic rate constants
$k_{r1,2,3}$ = reverse kinetic rate constants

REFERENCES

(1) Zeldovich, Y. B. The oxidation of nitrogen in combustion and explosions. *Acta Physicochim. URSS* **1946**, *21* (4), 577–628.

(2) Wendt, J. O. L.; Sternling, C. V.; Matovich, M. A. Reduction of sulfur trioxide and nitrogen oxides by secondary fuel injection. *Proc. Combust. Inst.* **1974**, *14*, 1085.

(3) Lv, Y.; Wang, Z.; Zhou, J.; Cen, K. Reduced mechanism for hybrid NO_x control process. *Energy Fuels* **2009**, *23* (12), 5920–5928.

(4) Dagaut, P.; Luche, J.; Cathonnet, M. The kinetics of C_1 to C_4 hydrocarbons/NO interactions in relation with reburning. *Symp. (Int.) Combust., [Proc.]* **2000**, *28* (2), 2459–2465.

(5) Frassoldati, A.; Faravelli, T.; Ranzi, E. Kinetic modeling of the interactions between NO and hydrocarbons at high temperature. *Combust. Flame* **2003**, *135* (1−2), 97–112.

(6) Miller, J. A.; Bowman, C. T. Mechanism and modeling of nitrogen chemistry in combustion. *Prog. Energy Combust. Sci.* **1989**, *15*, 287–338.

(7) Bowman, C. T. Control of combustion-generated nitrogen oxide emissions: Technology driven by regulation. *Symp. Int. Combust.* **1992**, *24* (1), 859–78.

(8) Smoot, L. D.; Hill, S. C.; Xu, H. NO_x control through reburning. *Prog. Energy Combust. Sci.* **1998**, *24* (5), 385–408.

(9) Maly, P. M.; Zamansky, V. M.; Ho, L.; Payne, R. Alternative fuel reburning. *Fuel* **1999**, *78* (3), 327–34.

(10) Rüdiger, H.; Kicherer, A.; Greul, U.; Spliethoff, H.; Hein, K. R. G. Investigations in combined combustion of biomass and coal in power plant technology. *Energy Fuels* **1996**, *10* (3), 789–96.

(11) Zarnitz, R.; Pisupati, S. V. Evaluation of the use of coal volatiles as reburning fuel for NO_x reduction. *Fuel* **2007**, *86* (4), 554–559.

(12) Singh, S.; Nimmo, W.; Gibbs, B. M.; Williams, P. T. Waste type rubber as a secondary fuel for power plants. *Fuel* **2009**, *88* (12), 2473–2480.

(13) Cancès, J.; Commandré, J. -M.; Salvador, S.; Dagaut, P. NO reduction capacity of four major solid fuels in reburning conditions experiments and modeling. *Fuel* **2008**, *87* (3), 274–289.

(14) Frederiksen, R. Fuel Lean Gas Reburn (FLGRTM) Technology for Achieving NO_x Emissions Compliance: Application to a Tangentially-Fired Boiler. 1998 Joint-American/Japanese Flame Research Committee International Symposium, 1998.

(15) Hura, H. S.; Breen, B. P., Gabrielson, J. E. Apparatus and method for NO_x reduction by selective injection of natural gas jets in flue gas. U.S. Patent 5,915,310, 1999.

(16) Miller, C. A.; Touati, A. D.; Becker, J.; Wendt, J. O. L. NO_x abatement by fuel-lean reburning: Laboratory combustor and pilot-scale package boiler results. *Symp. Int. Combust.* **1998**, *2*, 3189–95.

(17) Breen, B. P.; Hura, H. S. Method and apparatus for NO_x reduction in flue gases. U.S. Patent 6,258,336, 2001.

(18) Zheng, Y.; Fan, J.; Ma, Y.; Sun, P.; Cen, K. Computational modeling of tangentially fired boiler(II) NO_x emissions. *Chin. J. Chem. Eng.* **2000**, *8* (3), 247–50.

(19) Habib, M. A.; Elshafel, M.; Dajani, M. Influence of combustion parameters on NO_x production in an industrial boiler. *Comp. Fluids* **2008**, *37* (1), 12–23.

(20) Frassoldati, A.; Frigerio, S.; Colombo, E.; Inzoli, F.; Faravelli, T. Determination of NO_x emissions from strong swirling confined flames with an integrated CFD-based procedure. *Chem. Eng. Sci.* **2005**, *60* (11), 2851–2869.

(21) Kim, H. S.; Baek, S. W.; Yu, M. J. Formation characteristics of nitric oxide in a three-staged air/LPG flame. *Int. J. Heat Mass Transfer* **2003**, *46* (16), 2993–3008.

(22) Baek, S. W.; Kim, J. J.; Kim, H. S.; Kang, S. H. Effects of addition of solid particles on thermal characteristics in hydrogen-air flame. *Combust. Sci. Technol.* **2002**, *174* (8), 99–116.

(23) Gupta, A. K.; Lilly, D. G.; Syred, N. Swirl flows. *Swirl Flows;* Abacus press: Preston, U.K., 1984.

(24) Lee, C. Y.; Baek, S. W. Effects of hybrid reburning/SNCR strategy on NO_x/CO reduction and thermal characteristics in oxygen-enriched LPG flame. *Combust. Sci. Technol.* **2007**, *179* (8), 1649–66.

(25) Modest, M. F. *Radiative Heat Transfer*, 2nd ed.; Academic Press: New York, 2003.

(26) Zhou, W.; Moyeda, D.; Payne, R.; Berg, M. Application of numerical simulation and full scale testing for modeling low NO_X burner emissions. *Combust. Theory Modell.* **2009**, *13* (6), 1053–70.

(27) ANSYS, Inc. FLUENT 6.3 user guide; Canonsburg, PA, 2006.

(28) Hill, S. C.; Smoot, L. D. Modeling of nitrogen oxides formation and destruction in combustion systems. *Prog. Energy Combust. Sci.* **2000**, *26* (4), 417–58.

(29) Hanson, R. K.; Salimian, S. Survey of rate constants in H/NO/O systems. In *Combustion Chemistry*; Gardiner, W. C., Ed.; Springer: New York, 1984.

(30) Fenimore, C. P. Studies of fuel-nitrogen species in rich flame gases. *Symp. Int. Combust.* **1979**, *17* (1), 661–70.

(31) Kandamby, N.; Lazopoulos, G.; Lockwood, F. C.; Perera, A.; Vigevano, L. Mathematical modeling of NO_x emission reduction by the use of reburn technology in utility boilers. In ASME International Joint Power Generation Conference and Exhibition, Houston, TX, 1996.

(32) Su, S.; Xiang, J.; Sun, X.; Zhang, Z.; Zheng, C.; Xu, M. Mathematical modeling of nitric oxide destruction by reburning. *Energy Fuels* **2006**, *20* (4), 1434–1443.

(33) Hayhurst, A. N.; Parmar, M. S. Does solid carbon burn in oxygen to give the gaseous intermediate CO or produce CO_2 directly? Some experiments in a hot bed of sand fluidized by air. *Chem. Eng. Sci.* **1998**, *53* (3), 427–438.